
Multi-layer Learnable Attention Mask for Multimodal Tasks

Wayner Barrios
Dartmouth College

SouYoung Jin
Dartmouth College

Abstract

While the Self-Attention mechanism in the Transformer model has proven to be effective in many domains, we observe that it is less effective in more diverse settings (e.g. multimodality) due to the varying granularity of each token and the high computational demands of lengthy sequences. To address the challenges, we introduce the Learnable Attention Mask (LAM), strategically designed to globally regulate attention maps and prioritize critical tokens within the sequence. Leveraging the Self-Attention module in a BERT-like transformer network, our approach adeptly captures associations between tokens. The extension of the LAM to a multi-layer version accommodates the varied information aspects embedded at each layer of the Transformer network. Comprehensive experimental validation on various datasets, such as MADv2, QVHighlights, ImageNet 1K, and MSRVT, demonstrates the efficacy of the LAM, exemplifying its ability to enhance model performance while mitigating redundant computations. This pioneering approach presents a significant advancement in enhancing the understanding of complex scenarios, such as in movie understanding.

1 Introduction

The evolution of deep learning has empowered us to navigate increasingly complex scenarios, where many of which require digesting information from diverse sources, such as videos, images, audio, and text. One such scenario lies in understanding movie scenes [35, 13, 14, 3, 34, 41, 19, 5], where models aim to extract meaningful insights from multiple modalities.

Consider a movie scene represented by video and audio tokens. While these tokens naturally align in time, each one can be associated with any other tokens presented in the scene, as in Figure 1(a). While the Self-Attention module is effective for computing local associations between tokens, we have observed several drawbacks in the current attention mechanism, especially when tokens originate from diverse modalities. Firstly, different modalities introduce varying granularities of information, leading to potential challenges. Each token in one modality may be associated with multiple tokens in the other modality. Such associations can extend beyond one-to-one correspondences, forming between sub-sequences of tokens in each modality. In Figure 1(a), “Joanna’s shouts” might not be associated with a single video token but with several. Moreover, while longer sequence of tokens generally offers richer information, the computational demands of attention mechanisms increase with the input length of tokens. This constraint hinders the effective processing of a higher number of tokens.

Our method stems from the empirical observation that not all tokens in complex input sequences carry equal importance. While prior works like [9, 36, 28, 33] have demonstrated the effectiveness of dynamically updated masking mechanisms, this concept remains relatively unexplored in the computer vision domain, with only a few studies such as [27] delving into it. This gap in vision research has motivated our comprehensive analysis of the impact of dynamic token masking across diverse vision tasks.

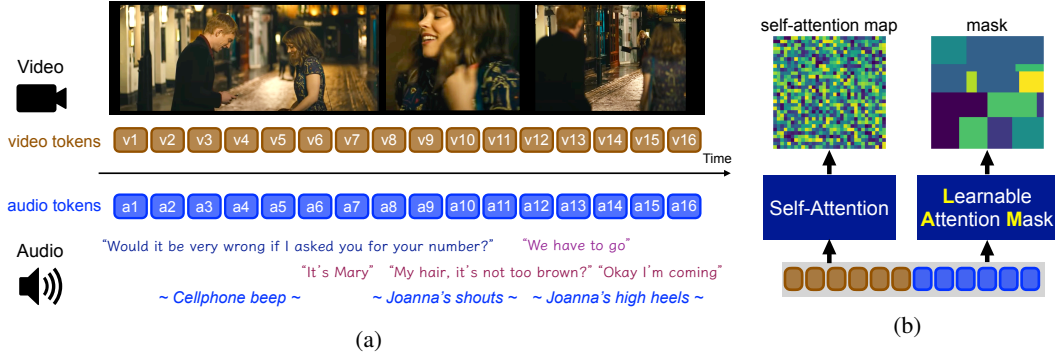


Figure 1: (a) While video and audio tokens naturally align in time, their associations can extend beyond temporal boundaries. For example, “Joanna’s shouts” may correspond to multiple video tokens (i.e. not just v8-11, but also v13-16). (b) The Self-Attention module [38] can capture these attention scores *locally*, token-versus-token. We introduce the Learnable Attention Mask (LAM), a novel concept that enables a holistic overview of the entire sequence of input tokens, generating a mask that captures attention structures *globally*.

To tackle the challenges posed by complex input sequences, we propose the **Learnable Attention Mask (LAM)** – a novel mechanism that dynamically generates masks to regulate attention maps and prioritize critical tokens based on their contextual significance. By processing the entire input sequence, LAM enables efficient token inspection and dynamic prioritization tailored to each sequence. This adaptive masking technique seamlessly integrates into existing Transformer Encoder architectures, offering a flexible solution to enhance transformer-based models across diverse applications. Given the widespread adoption of transformers, LAM’s plug-and-play nature could benefit researchers by enabling performance improvements through effortless integration.

The LAM method employs linear layers that take a complex token sequence as input, which can be either single-modal or multimodal. The output is a mask of size $L_t \times L_t$, where L_t represents the length of the input sequence T . The generated mask can be applied globally across all transformer layers in the stack, or it can be scaled individually for each transformer layer.

Eventually, the resulting mask, as illustrated in Figure 1(b), captures attention structures globally. This generated mask is then element-wise multiplied with the attention scores, allowing the masking out or prioritization of specific tokens. Furthermore, our observation that each layer in the Transformer Network embeds different information aspects motivates us to install the LAM module per stage, leading to the extension of the LAM to a multi-layer LAM.

We validate the effectiveness of our approach across various experimental settings. Initially, we assess the capability of the multi-layer LAM in multimodal settings, presenting results from audio description generation experiments on the MADv2 dataset [35, 13]. Additionally, we apply our approach to Moment Retrieval and Highlight Detection tasks on the QVHighlight dataset [24], incorporating both text and video inputs. Furthermore, we demonstrate that the LAM could enhance the performance in single-modality settings, such as image classification task in ImageNet 1K [8] and video captioning task in MSRVT [42] where a single modality is considered as input to the model. While the performance gain in single-modality settings is not significant, we demonstrate that our multi-layer LAM can be adopted in various scenarios. Finally, we analyze how the generated mask effectively regulates attention maps.

In summary, our contributions are **three-fold**:

1. We propose the Learnable Attention Mask (LAM), an innovative mechanism that dynamically identifies and prioritizes the most significant tokens within intricate input sequences. By generating masks that regulate attention maps, LAM ensures that the model’s focus is directed towards the critical tokens, optimizing performance on complex sequence processing tasks. With the widespread adoption of transformer architectures across various domains, the LAM’s modular design allows for seamless integration into existing transformer encoder frameworks. This plug-and-play capability presents a valuable opportunity for researchers to

leverage LAM’s token prioritization capabilities, potentially enhancing model performance with minimal effort and architectural modifications.

2. Through extensive experiments across various benchmarks, including MAD, ImageNet-1K, MSRVT, and QVHighlights, we empirically demonstrate the effectiveness of our LAM method, particularly when employed with multimodal encoders.
3. We analyze the output of the LAM and its influence on attention weight distributions, supplemented by qualitative analysis to provide insights into its behavior.

2 Related Work

2.1 Multimodal Transformers

A predominant area of prior exploration in aligning multiple modalities centers around contrastive learning, a method extensively utilized in both image-text and video-audio alignment contexts [6, 21, 32, 15, 12, 44]. Recent investigations have also delved into merging diverse modalities within a unified feature space through the incorporation of cross-attention layers [4, 23, 40, 30]. Furthermore, there is a growing trend of leveraging Transformer capabilities for multimodal fusion tasks [29, 20, 12, 3, 24]. Our decision to employ a multimodal transformer in our design is rooted in its unparalleled capability to integrate information across diverse modalities, thus fostering a more comprehensive understanding of the input data. Through the utilization of this unified architecture, we are enabled to effectively capture intricate interactions within the sequence, strategically prioritizing relevant cues based on their significance. In contrast to conventional methodologies that treat modalities in isolation, the multimodal transformer facilitates the seamless integration of contextual information, thereby yielding more coherent and nuanced representations.

2.2 Language Models for Video Description

To adapt a Large Language Model (LLM) for AD generation, we incorporate an adapter module. This module processes audiovisual features and transforms them into the feature space of our LLM. The concept of training an adapter module rather than finetuning the entire LLM to account for a new modality has been widely explored [43, 18], but the method most similar to ours is LLaMA-Adapter [45, 11]. LLaMA adapter, however, does not account for audio data. Our method follows that of LLaMA-Adapter closely, but changes the input feature space to include both audio and video features. The previous State-of-the-Art in our specific task (generating audio descriptions of movie clips) on the MAD dataset are the AutoAD models [13, 14]. We are able to generate comparable results with significantly less fine tuning and contextual information. Recent models have also achieved significant results in finding important moments in longer videos, but these contributions are not particularly relevant to ours because we focus on describing shorter video segments [24, 3]. Another recent result similar to ours is the Video-LLaMA model, which focuses on general purpose visual question answering but uses a Q-Former instead of an adapter module to fuse the visual, audio, and text modalities [44].

2.3 Masking Attention

In the field of Natural Language Processing, researchers have explored various methods of constructing attention masks, while also investigating their impact on transformer architectures [9, 36, 28, 33]. Conversely, this exploration has received limited attention in Computer Vision [25, 27]. Motivated by this disparity, our objective is to investigate this phenomenon, particularly in the context of multimodal data, and its implications for task performance. Unlike the approach proposed by SwinBert [27], which advocates for a sparse and learnable mask, our focus aligns more closely with the principles of Mask Attention Networks [9]. Instead of relying on a static mask matrix, which may restrict the model’s ability to capture local relationships effectively, we propose employing a Learnable Attention Mask (LAM). This adaptive mechanism aims to prioritize and regulate attention tokens within long sequences based on their contextual significance in a dynamic manner.

3 Learnable Attention Mask (LAM)

Our goal is to train a Learnable Attention Mask that effectively prioritizes and regulates tokens based on their significance within a complex sequence. This adaptable mechanism can be seamlessly incorporated into any of the existing Transformer Encoders. Figure 2 shows the overview of the LAM architecture.

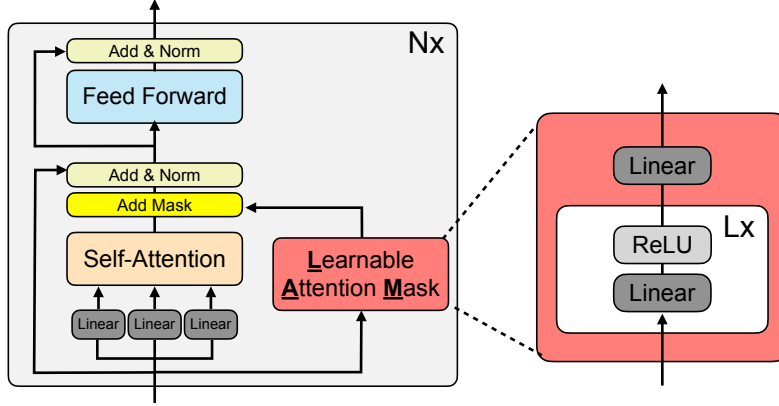


Figure 2: Overview of the Learnable Attention Mask Architecture. The Learnable Attention Mask (LAM) module takes the entire sequence as input and generates a mask. This mask is then used for element-wise multiplication with the attention scores produced by the Transformer Encoders.

3.1 Definition

We aim to generate an attention mask that adeptly prioritizes and regulates tokens according to their importance within a sequence. For this purpose, we develop a learnable module (denoted as \mathcal{X}), which receives a sequence of tokens T as input and returns a mask M , as shown in Equation 1. However, the shape of the mask M depends on the sequence length and the purpose of the multi-head attention, whether it's self-attention or cross-attention.

$$\mathcal{X}(T) \rightarrow M \quad (1)$$

Self-Attention. In the context of self-attention, the resulting mask output can be represented as $L_t \times L_t$, where L_t denotes the size of the input sequence T . Here, \mathcal{X} corresponds to a Feedforward network (FFN).

Cross-Attention. In cross-attention, \mathcal{X} will still be associated with a Feedforward network. Nonetheless, the function's input is determined by the dot product of the query Q and key K tensors within the multi-head attention layer, as indicated in Equation 2. Here, the shape of the mask M is defined as $L_q \times L_k$, where L_q is the length of the Query tensor and L_k the length of the Key tensor.

$$\mathcal{X}(QK^T) \rightarrow M \quad (2)$$

Scalability. This mask can be applied either globally across all transformer layers in a stack or scaled individually for each transformer layer within the stack. This flexibility enables the use of different masks depending on the depth of the layers.

3.2 Learnable Attention Mask Module

Let $\mathbf{x} \in \mathbb{R}^{d_{in}}$ denote the input to the Learnable Attention Mask module, and $\mathbf{W}_i \in \mathbb{R}^{d_{in_i} \times d_{out_i}}$, $\mathbf{b}_i \in \mathbb{R}^{d_{out_i}}$ be the weight matrix and bias vector of the i -th layer, respectively, where $i \in 1, 2, \dots, L$ and L is the total number of layers in LAM. The forward pass of the Learnable Attention Mask module is denoted as follows:

$$\mathbf{h}_1 = \text{ReLU}(\mathbf{W}_1 \mathbf{x} + \mathbf{b}_1) \quad (3)$$

$$\mathbf{h}_i = \text{ReLU}(\mathbf{W}_i \mathbf{h}_{i-1} + \mathbf{b}_i), \text{ for } i \in \{2, 3, \dots, L-1\} \quad (4)$$

$$M = \mathbf{W}_L \mathbf{h}_{L-1} + \mathbf{b}_L \quad (5)$$

where $\text{ReLU}(\cdot)$ represents the rectified linear unit activation function, and M denotes the generated mask.

3.3 Multi-Layer Learnable Attention Mask

In the context of the i^{th} layer of the self-attention Transformer, we denote the input sequence as $X^{(i)}$ and the resulting output as $Y^{(i)}$. Continuing with this notation, let’s delve into the mathematical representation of the attention mechanism within each layer:

$$\text{Att}^{(i)} = \text{softmax} \left(\frac{Q^{(i)}(X^{(i)})K^{(i)}(X^{(i)})^\top}{\sqrt{d_k}} \odot M^{(i)} \right) \quad (6)$$

Where $Q^{(i)}$ and $K^{(i)}$ represent the query, and key matrices respectively for the i^{th} layer. The mask $M^{(i)}$ is dynamically learned for each layer during training and adapts to the context within that layer, and \odot is a element-wise multiplication. The output $Y^{(i)}$ of the i^{th} layer serves as the input to the $(i+1)^{\text{th}}$ layer. Therefore, the attention mechanism changes for each layer due to the change in input. To show the change in mask and attention per layer, we need to consider the evolution of $X^{(i)}$ and $M^{(i)}$ as the layer index increases. The specific changes in attention and mask will depend on the architecture of the model and the learning process during training, with each layer potentially learning different attention patterns and mask distributions based on the evolving context of the input sequence.

3.4 Learnable Attention Mask for Cross Attention

The Learnable Mask Attention module, crucial to the cross-attention mechanism, utilizes Query and Key vectors as fundamental input components. It calculates the dot product between the Query vector Q and the transpose of the Key vector K^T to assess their mutual interaction. This dynamic interplay guides the allocation of focus, enabling the model to intelligently prioritize information extraction and processing across both sequences. By evaluating the dot product of the Query and Key vectors, the model gains valuable insights into their nuanced relationship. This understanding empowers the model to intelligently prioritize attention, ensuring optimal information extraction and processing across both sequences.

4 Experiments

4.1 Datasets

Generating AD. MADv2 [35, 13] is a vast dataset for video-language grounding, with over 264K queries in 488 movies totaling 892 hours. It includes MADv2-eval, with 10 movies for evaluation.

Moment Retrieval and Highlights Detection. QVHighlights [24] is the latest dataset for moment retrieval and highlight detection, featuring annotations for both tasks in over 10,000 YouTube videos.

Image Classification. ImageNet 1K [8] is a benchmark dataset consisting of 1.2 million images across 1,000 categories, commonly used for image classification tasks.

Video Captioning Task. MSRVT [42] is a dataset for video captioning, comprising 10,000 video clips from 20 categories with human-annotated descriptions.

4.2 Metrics

Generating AD. Conventional metrics like Rouge-L (R-L)[26], CIDEr (C)[39], and Retrieval-based metric (R@k/N) [14] are employed to compare generated Audio Descriptions (AD) with ground-truth AD. These metrics are robust to low-level variations in testing data, with higher values indicating superior text generation.

Moment Retrieval and Highlights Detection. For video grounding tasks, evaluation metrics include Recall@ K and mAP@ K for IoU= θ ($R@K$ -IoU= θ), assessing both ranking and temporal overlap. Models are evaluated at $K = 1$ with IoU thresholds of 0.5 and 0.7. Average mAP across IoU thresholds from 0.5 to 0.95 with 0.05 increments is calculated. Highlight detection primarily employs mAP, while HIT@1 measures the hit ratio for the highest scored clip.

Video Captioning. Evaluation metrics for video captioning include BLEU4 (B4) [31], CIDEr (C), SPICE (S) [1], METEOR (M) [22], and Rouge-L (R-L), capturing different aspects of caption quality such as n-gram overlap, semantic similarity, and linguistic fluency.

Image Classification. Performance in image classification is often measured using Accuracy top-1 (Acc-top1) and Accuracy top-5 (Acc-top5).

4.3 Baselines

We integrated our contribution into four baseline models: LLaMA AdapterV2 [11] with a transformer-based audiovisual encoder, QD-DETR [30], SwinBERT [27], and ViT Base [16, 38]. Our module, described in Section 3, was added **only** to the encoder of each model, except for SwinBERT, which follows its design principle by replacing the fixed learnable mask with our approach. For more details, see supplementary material.

Model	R-L	C	R@5/16
LlaMA [37, 11]	10.7	9.4	43.4
Ours	13.5	18.6	56.1
Gain(Δ)	2.8	9.2	12.7

(a) AD Task on MADv2-named [35, 13]

Model	R1@IoU0.7	mAP (Avg)
QD-DETR [30]	44.98	39.86
Ours	46.94	42.32
Gain(Δ)	1.96	2.46

(b) Moment Retrieval Task in QVHighlights [24]

Model	mAP	HIT@1
QD-DETR [30]	38.94	62.40
Ours	39.70	63.33
Gain(Δ)	0.76	0.93

(c) Highlights Detection at VeryGood confidence in QVHighlights [24]

Model	Acc-Top1	Acc-Top5
*ViT Base [16, 38]	82.71	96.32
Ours	83.45	96.59
Gain(Δ)	0.74	0.27

(d) Image Classification in ImageNet 1K [8]

Model	B4	R-L	M	C	S
SwinBERT [27]	42.82	62.06	30.39	51.96	7.64
Ours	42.03	62.05	30.60	52.24	8.03
Gain(Δ)	-0.79	-0.01	0.21	0.28	0.39

(e) Video Captioning Task in MSRVT [42]

Table 1: **Comparing performance across various datasets.** We evaluate our masking method on both multimodal encoders and single modality encoders. Our method demonstrates significant performance gains when applied to multimodal encoders, particularly in tasks (a, b, and c). However, for tasks involving single-modality encoders (d and e), we observe minimal improvements across most metrics. The asterisk (*) denotes that we retrained using the codebase and observed a slight decrease in performance compared to the numbers reported in [16].

4.4 Results

To examine the impact of our method, we evaluate its performance across five different tasks as presented in Table 1. Our analysis reveals that our method yields substantial improvements when applied to multimodal encoders compared to single-modality encoders. For instance, in Table 1a, we observe a maximum improvement of 12.7 for the R@5/16 metric, with an average improvement of 8.23 across all metrics. Similar trends are evident in Tables 1b and 1c, where maximum improvements

of 2.46 and 0.93, respectively, are observed alongside average improvements of 2.21 and 0.86, respectively. Conversely, when evaluating single-modality encoders, we generally observe minimal gains and occasional decreases in performance across certain metrics. For instance, in Table 1e, we note a decrease of 0.79 for the B4 metric, while slight increases of 0.28 and 0.39 are observed for the C and S metrics, respectively. Similarly, in Table 1d, a small improvement of 0.74 is observed for Acc-Top1.

Takeaway. Our method leverages multimodal sequences more effectively than single-modality sequences

Mask	R-L	C
Full Attention	12.92	15.46
Learnable Attn Mask (Fixed)*	10.02	9.72
Learnable Attn Mask	13.10	16.58
Multi-Layer Learnable Attn Mask	14.28	17.11

Table 2: **Attention Mask Influence.** We provide an analysis of the performance regarding the Audio Description generation task. Specifically, we utilized a subset comprising 1010 instances from the MADv2 (Supplementary Material). Our findings reveal an improvement in performance upon the integration of the Learnable Attention Mask module. Furthermore, we observed a slightly more pronounced enhancement with the incorporation of dynamic masks in each transformer layer (referred to as Multi-Layer Learnable Attention Mask). ‘*’ means we follow the learnable sparse mask design in [27]. Experiments were trained using the same hyper-parameters and 10 epochs.

4.5 Ablation Study

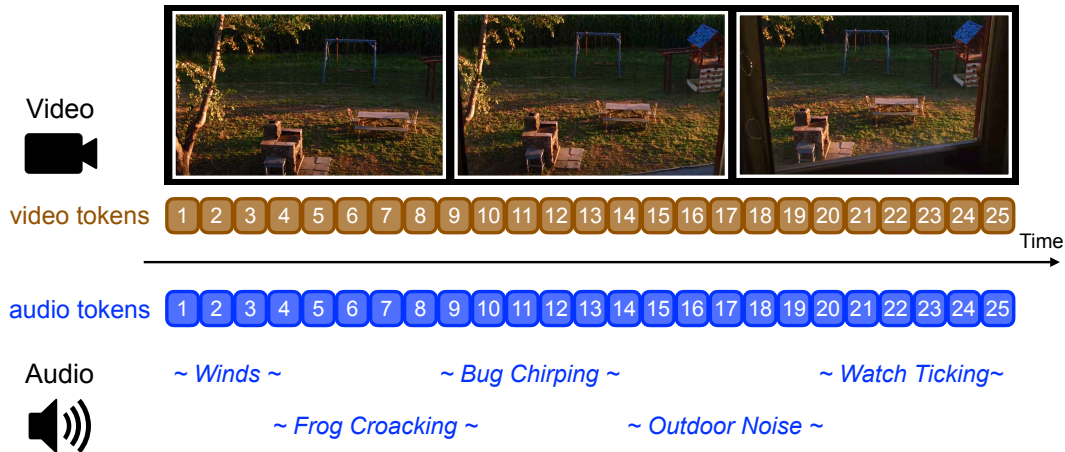
We investigate three crucial aspects of our Learnable Attention Mask (LAM) module’s design: **(i)** The representation capacity and depth of the attention mask itself, and how the depth of representing the mask impacts model performance. **(ii)** Whether the performance gains are primarily attributed to LAM’s masking and selective attention capabilities, or simply from having more trainable parameters. **(iii)** The optimal way to incorporate and fuse the learnable mask with the original attention map within the architecture. Through our analysis, we uncover design principles for effectively integrating LAM into the overall model to maximally leverage its selective attention capabilities. Understanding the interplay between attention mask representation depth, masking fusion strategies, model performance, and architectural factors provides insights into maximizing LAM’s efficacy for performance improvements.

Attention Mask Influence. We analyze the performance impact of the Learnable Attention Mask module using a subset of MAD-v2. We measure performance with Rouge-L and CIDEr metrics across four experiments: (i) full attention, (ii) learnable sparse mask from SwinBert, (iii) our Learnable Attention Mask (LAM), and (iv) Multi-Layer LAM. Employing LAM significantly improves performance over the full attention baseline, increasing CIDEr from 15.46 to 16.58. Multi-Layer LAM achieves the best performance at 17.11 CIDEr. In contrast, SwinBERT’s sparse learnable mask drops performance from 15.46 to 9.72 CIDEr due to its inability to capture the dynamic nature of MADv2 scenes with shot changes, transitions, and soundtracks. Our LAM better handles such multimodal sequences.

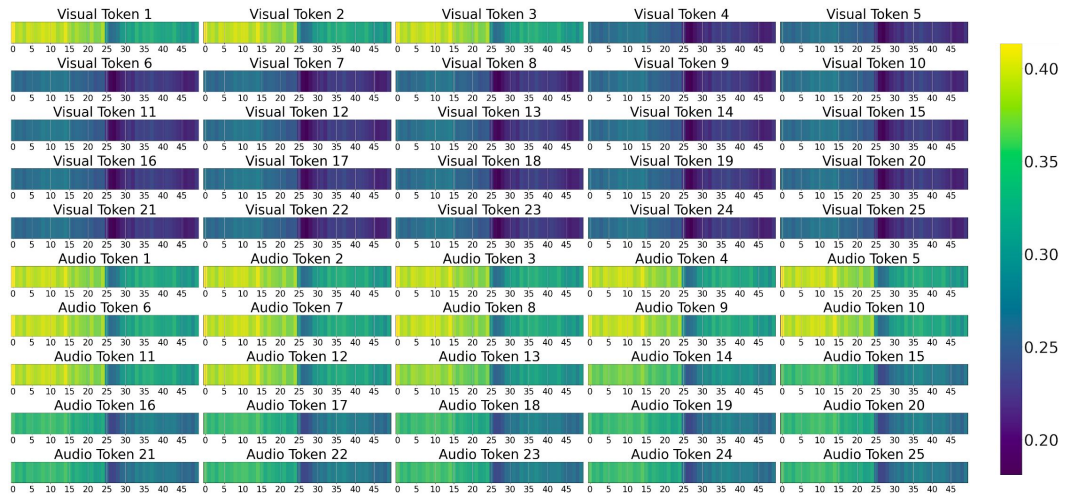
Experiment	R-L	C
Baseline	12.92	15.46
Full Attention w/ same number params.	11.23	12.87
Multi-Layer Learnable Attn Mask	14.28	17.11

Table 3: **Performance: Parameters vs. LAM Module Influence.** We present the performance results of three models: the baseline model without masking, a Full Attention Transformer with an equivalent number of parameters to the Multi-Layer Learnable Attention Mask, and the Multi-Layer Learnable Attention Mask itself. Generally, our findings suggest that the number of parameters does not directly correlate with performance gains.

Performance: Parameters vs. LAM Module Influence. We investigate whether the performance gains from our Learnable Attention Mask (LAM) module stem from the module itself or simply from increased model parameters. We compare a baseline model with full attention against a multi-layer LAM model and a variant model with full attention but additional linear layers to match the LAM model’s parameter count. Results on the audio description generation task (Table 3) show that merely increasing parameters without LAM leads to a drop in performance from 15.46 to 12.87 CIDEr. This suggests LAM’s efficacy comes from its ability to selectively emphasize token attention, not just added parameters.



(a) **Scene Visualization.** We highlight a specific moment from the movie Signs (2002) for qualitative analysis within the MADv2-eval set. Here, we meticulously present the visual elements while accurately representing the accompanying audio signals of the scene.



(b) **Scene Visualization** We also showcase the mask values produced by the Learnable Attention Mask (LAM) module for each visual and audio token present in the scene. These mask values exhibit positive numerical values, ranging between 0 and 1 inclusively.

Figure 3: **Qualitative Analysis.** This illustration presents a qualitative analysis of a specific instance from the MADv2-eval dataset. It depicts visual and audio signals alongside mask values corresponding to the initial transformer layer (1st layer). Video tokens are represented on the x-axis from 0 to 24, while audio tokens range from 25 to 50 on the same axis.

More Ablation Studies. In the supplementary material, you will find an analysis of how the depth (L number) impacts the performance of the LAM module. Additionally, it explores the effect of using two element-wise operations for masking fusion and how LAM modifies the distribution of attention weights.

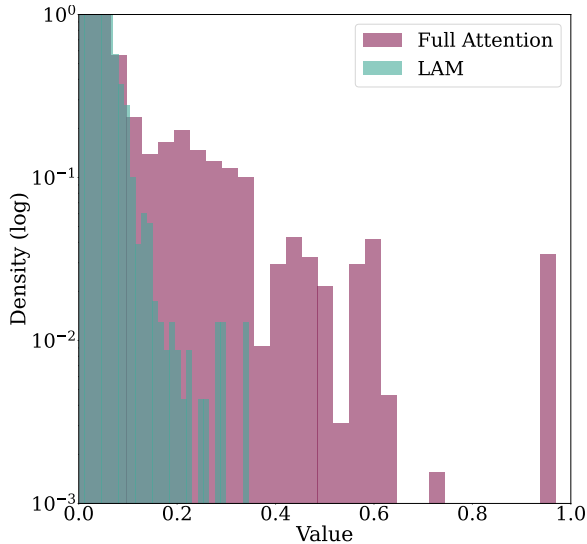


Figure 4: **Analysis of Attention Weight Distribution in the Qualitative Example.** The plot illustrates the distribution of attention weights within the initial transformer layer across two distinct configurations: employing Learnable Attention Mask (LAM) and full-attention mechanisms. It is evident from the depiction that attention weights under LAM tend to exhibit a leftward bias, resulting in a significant portion approaching 0 or nearing zero. The distribution weights correspond to the same example in Figure 3.

5 Qualitative Analysis

The qualitative analysis portrayed in Figure 3 provides insights into our implementation of Multi-Learnable Attention Mask (LAM) in the Audio Description generation task. The visual depiction highlights two aspects: Figure 3a shows the simultaneous audio and video signals, while Figure 3b illustrates the mask values corresponding to each token in the initial transformer layer. Despite slight zoom adjustments, the visual composition remains static, depicting the backyard of a house throughout all frames. Consequently, the LAM module activates only three visual tokens out of twenty-five, assigning minimal attention to the audio tokens. In contrast, the auditory elements exhibit captivating dynamics, transitioning from the sounds of wind, insects, and a frog to the rhythmic ticking of a clock. The ground truth Audio Description is: “A set of swings and a climbing frame stand in a rural backyard, along with a picnic table and a brick barbecue”. The model prioritizes attention to outdoor sounds (wind, insects, frog) over indoor sounds (watch ticking), aligning with visual token attention. Initial outdoor audio tokens strongly attend to first visual backyard tokens. Less attention is given to tokens related to transitioning indoors, coherent with describing the rural backyard. To compare with self-attention, Figure 4 shows attention weight distributions for Learnable Attention Mask (LAM) and full-attention on the same scene. Without LAM, the distribution is more uniform, suggesting more tokens receive attention. With LAM, the distribution is skewed left with many weights near zero, implying focused attention on fewer tokens. This analysis highlights LAM’s capability to discern and prioritize specific tokens, enhancing multimodal scene interpretation.

6 Conclusions and Limitations

In this work, we introduce the Learnable Attention Mask (LAM) as a novel solution to tackle challenges in attention mechanisms. The LAM enables models to embrace a comprehensive perspective of the entire input, eventually regulating attention maps, prioritizing critical tokens, and reducing unnecessary computations. While our model demonstrates significant improvements in multimodal settings, we recognize the potential for further enhancement through the inclusion of additional contextual information during inference, such as character names for AD task. Additionally, we observe that the gains are not as significant in single-modality settings. Nevertheless, we believe that our proposed approach and experimental results will serve as a foundational stepping stone for future research in understanding and applying attention mechanisms across various scenarios.

References

- [1] Peter Anderson, Basura Fernando, Mark Johnson, and Stephen Gould. SPICE: semantic propositional image caption evaluation. In Bastian Leibe, Jiri Matas, Nicu Sebe, and Max Welling, editors, *Computer Vision - ECCV 2016 - 14th European Conference, Amsterdam, The Netherlands, October 11-14, 2016, Proceedings, Part V*, volume 9909 of *Lecture Notes in Computer Science*, pages 382–398. Springer, 2016. doi: 10.1007/978-3-319-46454-1_24. URL https://doi.org/10.1007/978-3-319-46454-1_24.
- [2] Relja Arandjelovic and Andrew Zisserman. Look, listen and learn. In *2017 IEEE International Conference on Computer Vision (ICCV)*, pages 609–617, 2017. doi: 10.1109/ICCV.2017.73.
- [3] Wayner Barrios, Mattia Soldan, Alberto Mario Ceballos-Arroyo, Fabian Caba Heilbron, and Bernard Ghanem. Localizing moments in long video via multimodal guidance. In *Proceedings of the IEEE/CVF International Conference on Computer Vision (ICCV)*, pages 13667–13678, October 2023.
- [4] C. Chen, Q. Fan, and R. Panda. Crossvit: Cross-attention multi-scale vision transformer for image classification. In *2021 IEEE/CVF International Conference on Computer Vision (ICCV)*, pages 347–356, Los Alamitos, CA, USA, oct 2021. IEEE Computer Society. doi: 10.1109/ICCV48922.2021.00041. URL <https://doi.ieeecomputersociety.org/10.1109/ICCV48922.2021.00041>.
- [5] Shixing Chen, Chun-Hao Liu, Xiang Hao, Xiaohan Nie, Maxim Arap, and Raffay Hamid. Movies2scenes: Using movie metadata to learn scene representation. In *Proceedings of the IEEE/CVF Conference on Computer Vision and Pattern Recognition (CVPR)*, pages 6535–6544, June 2023.
- [6] Ting Chen, Simon Kornblith, Mohammad Norouzi, and Geoffrey E. Hinton. A simple framework for contrastive learning of visual representations. *ArXiv*, abs/2002.05709, 2020. URL <https://api.semanticscholar.org/CorpusID:211096730>.
- [7] Jason Cramer, Ho-Hsiang Wu, Justin Salamon, and Juan Pablo Bello. Look, listen, and learn more: Design choices for deep audio embeddings. In *ICASSP 2019 - 2019 IEEE International Conference on Acoustics, Speech and Signal Processing (ICASSP)*, pages 3852–3856, 2019. doi: 10.1109/ICASSP.2019.8682475.
- [8] Jia Deng, Wei Dong, Richard Socher, Li-Jia Li, K. Li, and Li Fei-Fei. Imagenet: A large-scale hierarchical image database. *2009 IEEE Conference on Computer Vision and Pattern Recognition*, pages 248–255, 2009. URL <https://api.semanticscholar.org/CorpusID:57246310>.
- [9] Zhihao Fan, Yeyun Gong, Dayiheng Liu, Zhongyu Wei, Siyuan Wang, Jian Jiao, Nan Duan, Ruofei Zhang, and Xuanjing Huang. Mask attention networks: Rethinking and strengthen transformer. In Kristina Toutanova, Anna Rumshisky, Luke Zettlemoyer, Dilek Hakkani-Tur, Iz Beltagy, Steven Bethard, Ryan Cotterell, Tanmoy Chakraborty, and Yichao Zhou, editors, *Proceedings of the 2021 Conference of the North American Chapter of the Association for Computational Linguistics: Human Language Technologies*, pages 1692–1701, Online, June 2021. Association for Computational Linguistics. doi: 10.18653/v1/2021.naacl-main.135. URL <https://aclanthology.org/2021.naacl-main.135>.
- [10] Christoph Feichtenhofer, Haoqi Fan, Jitendra Malik, and Kaiming He. Slowfast networks for video recognition. *2019 IEEE/CVF International Conference on Computer Vision (ICCV)*, pages 6201–6210, 2018.
- [11] Peng Gao, Jiaming Han, Renrui Zhang, Ziyi Lin, Shijie Geng, Aojun Zhou, Wei Zhang, Pan Lu, Conghui He, Xiangyu Yue, Hongsheng Li, and Yu Qiao. Llama-adapter v2: Parameter-efficient visual instruction model. *arXiv preprint arXiv:2304.15010*, 2023.
- [12] Jiaming Han, Renrui Zhang, Wenqi Shao, Peng Gao, Peng Xu, Han Xiao, Kaipeng Zhang, Chris Liu, Song Wen, Ziyu Guo, Xudong Lu, Shuai Ren, Yafei Wen, Xiaoxin Chen, Xiangyu Yue, Hongsheng Li, and Yu Qiao. Imagebind-llm: Multi-modality instruction tuning, 2023.

- [13] Tengda Han, Max Bain, Arsha Nagrani, Gül Varol, Weidi Xie, and Andrew Zisserman. AutoAD: Movie description in context. In *CVPR*, 2023.
- [14] Tengda Han, Max Bain, Arsha Nagrani, Gül Varol, Weidi Xie, and Andrew Zisserman. AutoAD II: The Sequel - who, when, and what in movie audio description. In *ICCV*, 2023.
- [15] Kaiming He, Haoqi Fan, Yuxin Wu, Saining Xie, and Ross B. Girshick. Momentum contrast for unsupervised visual representation learning. *2020 IEEE/CVF Conference on Computer Vision and Pattern Recognition (CVPR)*, pages 9726–9735, 2019. URL <https://api.semanticscholar.org/CorpusID:207930212>.
- [16] Kaiming He, Xinlei Chen, Saining Xie, Yanghao Li, Piotr Dollár, and Ross B. Girshick. Masked autoencoders are scalable vision learners. *2022 IEEE/CVF Conference on Computer Vision and Pattern Recognition (CVPR)*, pages 15979–15988, 2021.
- [17] J. Edward Hu, Yelong Shen, Phillip Wallis, Zeyuan Allen-Zhu, Yuanzhi Li, Shean Wang, and Weizhu Chen. Lora: Low-rank adaptation of large language models. *ArXiv*, abs/2106.09685, 2021. URL <https://api.semanticscholar.org/CorpusID:235458009>.
- [18] Zhiqiang Hu, Yihuai Lan, Lei Wang, Wanyu Xu, Ee-Peng Lim, Roy Ka-Wei Lee, Lidong Bing, and Soujanya Poria. Llm-adapters: An adapter family for parameter-efficient fine-tuning of large language models. *arXiv preprint arXiv:2304.01933*, 2023.
- [19] Md Mohaiminul Islam, Mahmudul Hasan, Kishan Shamsundar Athrey, Tony Braskich, and Gedas Bertasius. Efficient movie scene detection using state-space transformers. In *Proceedings of the IEEE/CVF Conference on Computer Vision and Pattern Recognition (CVPR)*, pages 18749–18758, June 2023.
- [20] Aishwarya Kamath, Mannat Singh, Yann LeCun, Ishan Misra, Gabriel Synnaeve, and Nicolas Carion. Mdetr - modulated detection for end-to-end multi-modal understanding. *2021 IEEE/CVF International Conference on Computer Vision (ICCV)*, pages 1760–1770, 2021.
- [21] Prannay Khosla, Piotr Teterwak, Chen Wang, Aaron Sarna, Yonglong Tian, Phillip Isola, Aaron Maschiot, Ce Liu, and Dilip Krishnan. Supervised contrastive learning. *arXiv preprint arXiv:2004.11362*, 2020.
- [22] Alon Lavie and Abhaya Agarwal. Meteor: an automatic metric for mt evaluation with high levels of correlation with human judgments. In *Proceedings of the Second Workshop on Statistical Machine Translation, StatMT '07*, page 228–231, USA, 2007. Association for Computational Linguistics.
- [23] Jun-Tae Lee, Mihir Jain, Hyoungwoo Park, and Sungrack Yun. Cross-attentional audio-visual fusion for weakly-supervised action localization. In *International Conference on Learning Representations*, 2021. URL <https://api.semanticscholar.org/CorpusID:235614339>.
- [24] Jie Lei, Tamara L Berg, and Mohit Bansal. Detecting moments and highlights in videos via natural language queries. In M. Ranzato, A. Beygelzimer, Y. Dauphin, P.S. Liang, and J. Wortman Vaughan, editors, *Advances in Neural Information Processing Systems*, volume 34, pages 11846–11858. Curran Associates, Inc., 2021. URL <https://proceedings.neurips.cc/paper/2021/file/62e0973455fd26eb03e91d5741a4a3bb-Paper.pdf>.
- [25] Zhaowen Li, Zhiyang Chen, Fan Yang, Wei Li, Yousong Zhu, Chaoyang Zhao, Rui Deng, Liwei Wu, Rui Zhao, Ming Tang, and Jinqiao Wang. Mst: Masked self-supervised transformer for visual representation. In M. Ranzato, A. Beygelzimer, Y. Dauphin, P.S. Liang, and J. Wortman Vaughan, editors, *Advances in Neural Information Processing Systems*, volume 34, pages 13165–13176. Curran Associates, Inc., 2021. URL https://proceedings.neurips.cc/paper_files/paper/2021/file/6dbbe6abe5f14af882ff977fc3f35501-Paper.pdf.
- [26] Chin-Yew Lin. ROUGE: A package for automatic evaluation of summaries. In *Text Summarization Branches Out*, pages 74–81, Barcelona, Spain, July 2004. Association for Computational Linguistics. URL <https://aclanthology.org/W04-1013>.

- [27] Kevin Lin, Linjie Li, Chung-Ching Lin, Faisal Ahmed, Zhe Gan, Zicheng Liu, Yumao Lu, and Lijuan Wang. Swinbert: End-to-end transformers with sparse attention for video captioning. In *CVPR*, 2022.
- [28] Te Lin and Inwhae Joe. An adaptive masked attention mechanism to act on the local text in a global context for aspect-based sentiment analysis. *IEEE Access*, 11:43055–43066, 2023. doi: 10.1109/ACCESS.2023.3270927.
- [29] Huaishao Luo, Lei Ji, Ming Zhong, Yang Chen, Wen Lei, Nan Duan, and Tianrui Li. Clip4clip: An empirical study of clip for end to end video clip retrieval. *arXiv preprint arXiv:2104.08860*, 2021.
- [30] WonJun Moon, Sangeek Hyun, SangUk Park, Dongchan Park, and Jae-Pil Heo. Query-dependent video representation for moment retrieval and highlight detection. In *Proceedings of the IEEE/CVF Conference on Computer Vision and Pattern Recognition*, pages 23023–23033, 2023.
- [31] Kishore Papineni, Salim Roukos, Todd Ward, and Wei-Jing Zhu. Bleu: a method for automatic evaluation of machine translation. In *Proceedings of the 40th Annual Meeting on Association for Computational Linguistics, ACL '02*, page 311–318, USA, 2002. Association for Computational Linguistics. doi: 10.3115/1073083.1073135. URL <https://doi.org/10.3115/1073083.1073135>.
- [32] Alec Radford, Jong Wook Kim, Chris Hallacy, Aditya Ramesh, Gabriel Goh, Sandhini Agarwal, Girish Sastry, Amanda Askell, Pamela Mishkin, Jack Clark, Gretchen Krueger, and Ilya Sutskever. Learning transferable visual models from natural language supervision. In *International Conference on Machine Learning*, 2021. URL <https://api.semanticscholar.org/CorpusID:231591445>.
- [33] Riccardo Rende, Federica Gerace, Alessandro Laio, and Sebastian Goldt. What does self-attention learn from masked language modelling?, 2024.
- [34] Anna Rohrbach, Marcus Rohrbach, Niket Tandon, and Bernt Schiele. A dataset for movie description. *2015 IEEE Conference on Computer Vision and Pattern Recognition (CVPR)*, pages 3202–3212, 2015. URL <https://api.semanticscholar.org/CorpusID:15184723>.
- [35] Mattia Soldan, Alejandro Pardo, Juan León Alcázar, Fabian Caba, Chen Zhao, Silvio Giancola, and Bernard Ghanem. Mad: A scalable dataset for language grounding in videos from movie audio descriptions. In *Proceedings of the IEEE/CVF Conference on Computer Vision and Pattern Recognition (CVPR)*, pages 5026–5035, June 2022.
- [36] Jingfan Tang, Xinqiang Wu, Min Zhang, Xiujie Zhang, and Ming Jiang. Multiway dynamic mask attention networks for natural language inference. *J. Comp. Methods in Sci. and Eng.*, 21(1):151–162, jan 2021. ISSN 1472-7978. doi: 10.3233/JCM-204451. URL <https://doi.org/10.3233/JCM-204451>.
- [37] Hugo Touvron, Thibaut Lavril, Gautier Izacard, Xavier Martinet, Marie-Anne Lachaux, Timothée Lacroix, Baptiste Rozière, Naman Goyal, Eric Hambro, Faisal Azhar, Aurelien Rodriguez, Armand Joulin, Edouard Grave, and Guillaume Lample. Llama: Open and efficient foundation language models. *ArXiv*, abs/2302.13971, 2023. URL <https://api.semanticscholar.org/CorpusID:257219404>.
- [38] Ashish Vaswani, Noam Shazeer, Niki Parmar, Jakob Uszkoreit, Llion Jones, Aidan N Gomez, Łukasz Kaiser, and Illia Polosukhin. Attention is all you need. In I. Guyon, U. Von Luxburg, S. Bengio, H. Wallach, R. Fergus, S. Vishwanathan, and R. Garnett, editors, *Advances in Neural Information Processing Systems*, volume 30. Curran Associates, Inc., 2017. URL https://proceedings.neurips.cc/paper_files/paper/2017/file/3f5ee243547dee91fbd053c1c4a845aa-Paper.pdf.
- [39] Ramakrishna Vedantam, C. Lawrence Zitnick, and Devi Parikh. Cider: Consensus-based image description evaluation. *2015 IEEE Conference on Computer Vision and Pattern Recognition (CVPR)*, pages 4566–4575, 2014. URL <https://api.semanticscholar.org/CorpusID:9026666>.

- [40] Xi Wei, Tianzhu Zhang, Yan Li, Yongdong Zhang, and Feng Wu. Multi-modality cross attention network for image and sentence matching. In *2020 IEEE/CVF Conference on Computer Vision and Pattern Recognition (CVPR)*, pages 10938–10947, 2020. doi: 10.1109/CVPR42600.2020.01095.
- [41] Fanyi Xiao, Kaustav Kundu, Joseph Tighe, and Davide Modolo. Hierarchical self-supervised representation learning for movie understanding. In *Proceedings of the IEEE/CVF Conference on Computer Vision and Pattern Recognition (CVPR)*, pages 9727–9736, June 2022.
- [42] Jun Xu, Tao Mei, Ting Yao, and Yong Rui. Msr-vtt: A large video description dataset for bridging video and language. *2016 IEEE Conference on Computer Vision and Pattern Recognition (CVPR)*, pages 5288–5296, 2016.
- [43] Mohit Bansal Yi-Lin Sung, Jaemin Cho. V1-adapter: Parameter-efficient transfer learning for vision-and-language tasks. In *CVPR*, 2022.
- [44] Hang Zhang, Xin Li, and Lidong Bing. Video-llama: An instruction-tuned audio-visual language model for video understanding, 2023.
- [45] Renrui Zhang, Jiaming Han, Chris Liu, Peng Gao, Aojun Zhou, Xiangfei Hu, Shilin Yan, Pan Lu, Hongsheng Li, and Yu Qiao. Llama-adapter: Efficient fine-tuning of language models with zero-init attention. *arXiv preprint arXiv:2303.16199*, 2023.
- [46] Tianyi Zhang, Varsha Kishore, Felix Wu, Kilian Q. Weinberger, and Yoav Artzi. Bertscore: Evaluating text generation with BERT. In *8th International Conference on Learning Representations, ICLR 2020, Addis Ababa, Ethiopia, April 26-30, 2020*. OpenReview.net, 2020. URL <https://openreview.net/forum?id=SkeHuCVFDr>.

A Multimodal Encoder Tasks

We evaluated the effectiveness of the learnable mask attention across three significant multimodal tasks: Audio Description (AD) Generation, Moment Retrieval, and Highlights Detection. In this section, we first provide details in these tasks (Sections A.1 and A.2) and show the application of our proposed LAM module to each task (Sections A.3 and A.4).

A.1 Audio Description Generation

Our task involves adapting a Large Language Model (LLM) to generate Audio Descriptions (AD) in text for a long-form movie \mathcal{L} segmented into short clips $\{c_1, c_2, \dots, c_N\}$. Each clip encompasses \mathcal{S} samples in the visual stream (represented as V) and \mathcal{S} samples in the audio stream (denoted as A)¹. Specifically, our goal is to create a text t_i that describes the audiovisual content presented in each clip c_i , aiming to assist individuals who are blind in following the movie’s narrative.

Audiovisual Model \mathcal{AV} . We aim to train an audiovisual model that comprehends the relationships between sequential video and audio streams. Consequently, \mathcal{AV} processes video (V) and audio (A) observations sampled at c_i clip and produces an audiovisual feature representations E_{va} .

$$\mathcal{AV}(V, A) \rightarrow E_{va} \tag{7}$$

Large Language Model \mathcal{H} . Given an input sequence $X = \{x_1, x_2, \dots, x_n\}$, the model \mathcal{H} estimates the probability distribution of the next word x_{n+1} based on the context using the chain rule of probability:

$$P(x_{n+1}|X) = P(x_{n+1}|x_1, x_2, \dots, x_n) \tag{8}$$

The model is trained by maximizing the likelihood of generating the correct sequence according to the training data. During inference, it predicts the most likely next word given the context. The model’s

¹Raw sound from movies, excluding descriptions

weights θ are optimized through back-propagation and gradient descent to improve its language understanding and generation capabilities.

Adapter Module \mathcal{P} . Let’s assume a pre-trained model with parameters represented by θ . The adapter layer introduces additional parameters for audiovisual understanding task, and these parameters can be denoted as ϕ . The output of the adapter layers can be represented as $P(x', \phi)$, where x' is the projected audiovisual features into the language space. So, the overall output of the model with the adapter layer can be written as:

$$\mathcal{F}(\mathcal{H}(x, \theta), \mathcal{P}(x', \phi)) \rightarrow t_i \quad (9)$$

Where \mathcal{F} is a function that combines the pre-trained Language Model \mathcal{H} and the adapter \mathcal{P} to produce an AD in text t_i .

A.2 Moment Retrieval and Highlights detection

The visual-language grounding model, denoted as \mathcal{G} , is tasked with processing an untrimmed video, V , sampled from a temporal window W , along with a natural language query Q . It then produces predictions for J temporal moments, defined as:

$$\mathcal{G}(V, Q) \rightarrow (\tau_s, \tau_e, s, s_l)_1^J. \quad (10)$$

In Equation 10, the grounding models yield a series of moments ranked by their confidence scores. Here, (τ_s, τ_e) represents the duration span of the moment, while s indicates its confidence score. Now, let’s define the inputs for our attention modules. Given a video comprising L clips and a text query containing N words, their representations extracted by frozen video and text encoders are denoted as v_1, v_2, \dots, v_L and t_1, t_2, \dots, t_N , respectively. Additionally, the grounding model provides saliency scores s_l for each moment for the highlight detection task.

A.3 Implementation Details for AD Generation

Feature Extraction. The extraction of visual features follows the CLIP-based methodology outlined in [35]. To be more specific, visual features are extracted at a rate of 5 frames per second (FPS) with an embedding dimensionality of $D_v=512$. For audio feature extraction, we follow [3] by utilizing the OpenL3 [7, 2] checkpoint pre-trained on videos containing environmental audiovisual data. We use a spectrogram time-frequency representation with 128 bands and set the audio embedding dimensionality D_a to 512. Furthermore, we extract the audio embeddings using a stride size of 0.2 seconds, *i.e.*, with an extraction frame rate of 5 Hz, matching the frame rate of the visual features.

Audiovisual Model \mathcal{AV} . We utilize a Multimodal Transformer with a standard configuration [38]. For each observation c_i , consisting of both visual and audio information, we employ $S = 25$ visual tokens and $S = 25$ audio tokens, effectively spanning a 5-second duration at a frame rate of 5 FPS. This Multimodal Transformer architecture comprises 16 layers and employs a Multi-Layer Learnable Attention Mask with a dimensionality of 768.

Large Language Model \mathcal{H} . For Large Language Model, we choose to employ a frozen LLaMA 7B model [37] and opt to use its official checkpoint.

Adapter Module \mathcal{P} . We build our audiovisual adapter following the approach done in [11]. In this part, we select 16 tokens as audiovisual tokens. We adjust the last 31 layers of LLaMA 7B, making sure that the audiovisual features stay at a size of 512, which then maps to 4096 (LLaMA dimensionality). We set the depth to 8, use 16 heads, apply LoRA Rank [17] with a value of 16, and activate Bias layers [45].

Training Protocol. To generate Audio Descriptions, we follow the training methodology outlined in [45, 11]. This involved utilizing 8 RTX 6000 Ada Generation GPUs, each equipped with 50 GB VRAM, alongside employing a base learning rate of $1e - 4$ and the Adam optimizer.

A.4 Implementation Details for Moment Retrieval and Highlighting Task

Feature Extraction. The visual and text embeddings are extracted following the methodology presented in [24]. For video, we use SlowFast [10] and the visual encoder (ViT-B/32) of CLIP [32] to extract features every 2 seconds. We then normalize the two features and concatenate them at hidden dimension. The resulting visual features is denoted as $E_V \in \mathbb{R}^{L_V \times D_V}$, with $D_V = 2816$. For text features, we use the CLIP text encoder to extract token level features, $E_Q \in \mathbb{R}^{L_Q \times D_Q}$ with $D_Q = 512$.

Video Grounding Model. We adopt the methodology outlined in [30]. The architecture consists of three distinct components: an encoder comprising four layers of transformer blocks (two cross-attention layers and two self-attention layers), while the decoder has only two layers. We configure the hidden dimension of the transformers to be 256. Additionally, for the transformer encoder layers and the cross-attention layers, we utilize our Learnable Mask Attention method as detailed in Section 3.

Training Protocol. We conducted training over 200 epochs, employing a batch size of 32 and a learning rate set to $1e-4$. We utilized the Adam optimizer with a weight decay of $1e-4$, leveraging a single GPU, the RTX 6000 Ada Generation.

B Single Modality Encoder Tasks

B.1 Image Classification Task

In the image classification task, the goal is to assign an input image I to one or more predefined classes from a set of C classes. Let's denote the image classification model as \mathcal{M} . Given an input image I , the model generates a set of class predictions and their corresponding confidence scores:

$$\mathcal{M}(I) \rightarrow (\hat{y}_1, \hat{p}_1), (\hat{y}_2, \hat{p}_2), \dots, (\hat{y}_C, \hat{p}_C) \quad (11)$$

Here, $\hat{y}_c \in 1, 2, \dots, C$ represents the predicted class label for the c -th class, and $\hat{p}_c \in [0, 1]$ is the corresponding confidence score or probability assigned by the model to that class. The model's goal is to accurately predict the true classes present in the input image I .

B.2 Video Captioning Task

In the video captioning task, the goal is to generate a textual description or caption for a given input video V . Let's denote the video captioning model as \mathcal{M} . Given an input video V , the model generates a sequence of words $W = w_1, w_2, \dots, w_N$ that forms the caption:

$$\mathcal{M}(V) \rightarrow W = w_1, w_2, \dots, w_N \quad (12)$$

Here, each w_i represents a word in the generated caption, and N is the length of the caption sequence. The model's objective is to produce a natural language caption W that accurately and coherently describes the content and events depicted in the input video V .

B.3 Implementations Details for Image Classification Task

We follow the pre-trained model developed in [16] and fine-tune it for the image classification task. The base model is a Vision Transformer (ViT) with a 16x16 patch size, 768-dimensional embedding, 12 transformer layers, and 12 attention heads. It includes an MLP ratio of 4, biases in the query, key, and value projections, and layer normalization with an epsilon of $1e-6$. To incorporate our proposed Learnable Attention Mask (LAM) module, we use the Multi-LAM variant, which generates the attention mask using a single linear layer without ReLU activation. For the pretraining stage, we adhere to the methodology outlined in [16], but increase the batch size to 128 and use 4 gradient accumulation steps. For fine-tuning on the image classification task, we maintain a batch size of 128 and 4 gradient accumulation steps. Additionally, we train for 100 epochs, apply a weight decay of 0.05, set the drop path rate to 0.1, and use mixup and cutmix with values of 0.8 and 1.0, respectively.

B.4 Implementations Details for Video Captioning Task

We adopt the methodology proposed by SwinBERT [27], with a notable modification. Instead of using a fixed learnable mask implemented via `nn.Parameter`, we integrate our Learnable Attention

Mask (LAM) module, which consists of 16 layers while maintaining the same dimensionality as the original SwinBERT. Regarding the hyperparameters, the experiment utilizes a batch size of 2 per GPU, running for 20 epochs with a learning rate of 0.0003. Training is conducted in half precision using DeepSpeed, with gradient accumulation over 16 steps. The setup employs 8 A6000 Ada generation GPUs, ensuring efficient and powerful computational performance.

C Ablation Study

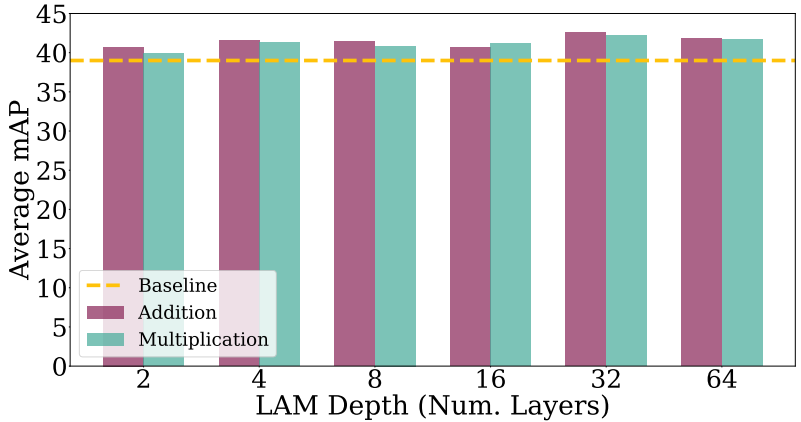


Figure S5: **Ablation Studies on the number of layers in LAM and types of mask operation.** We conduct an investigation into the impact of varying the number of layers utilized within the Learnable Attention Mask (LAM) framework, as applied in the cross-attention configuration, along with the methods employed for mask fusion with attention weights. The experimentation involves the manipulation of the number of layers, ranging from 2 to 64, and explores two distinct fusion techniques: multiplication and addition operations, both implemented at the element-wise level. Evaluation of these experiments is carried out on the validation split set of QVHighlights [24]. Overall, notable enhancements in performance, particularly concerning the Average mAP metric for the Moment Retrieval task, are observed. The most substantial improvements are achieved when utilizing 32 layers within the LAM module.

C.1 Influence of the Depth and Masking Fusion

In our experimental exploration of the cross-attention setup, we employ an ablation analysis to systematically assess the effects of removing two key components from the Learnable Attention Mask (LAM) module. These components encompass both the variation in the number of layers within the LAM module, as outlined in Section 3 of the main paper, and the distinct functionalities of mask operations: addition and multiplication. Figure S5 presents a detailed analysis of the performance outcomes achieved through the Average mAP metric for the Moment Retrieval task on the QVHighlights validation dataset. Delving deeper into the results, it is apparent that the utilization of LAM (Learnable Attention Mask) contributes to notable enhancements in performance. These improvements vary across different configurations, with some showcasing more substantial gains than others. Nevertheless, regardless of the specific layer types employed or the operations conducted, the results consistently surpass the baseline performance. Remarkably, in this particular examination, the most favorable outcomes were attained by employing 32 layers combined with both addition and multiplication operations. These configurations yielded impressive Average mAP metrics of 42.61 and 42.32 respectively, underscoring the efficacy of this approach in enhancing the performance of the Moment Retrieval task on the QVHighlights validation set.

Takeaway. While we mentioned in Section 3 of the main paper that the mask is integrated through element-wise multiplication, we also provide the option to incorporate addition at the element-wise level.

C.2 Attention Weights.

Figure S6 illustrates the attention weight distribution across three layers in the Transformer Network: the 1st, 8th, and the last layer, under both full-attention settings and utilizing Multi-Layer Learnable

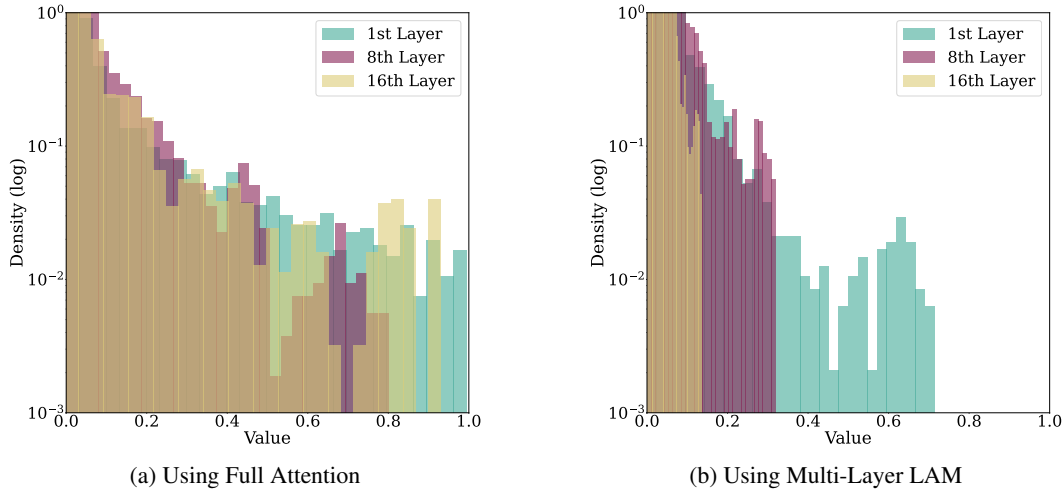


Figure S6: **Attention Weight Distribution.** We investigate the impact of our Learnable Attention Mask (LAM) on attention weight distribution during AD generation task. Utilizing LAM, attention weights decrease in value as they traverse deeper layers, with many approaching zero. This enhances efficiency in model training by reducing unnecessary computations. The attention weights were collected by doing forward pass of 64 samples.

Attention Mask (LAM). Notably, with our Multi-Layer LAM, a significant portion of attention weights diminishes to zero, while others converge towards values close to zero. This observation suggests that LAM has the potential to optimize the model training by minimizing redundant computations.

D Additional Details for Audio Description Generation

In the following sections, we examine specific details that have not been addressed in the main paper. This comprehensive discussion includes insights into the current methodology for calculating metrics, the specific prompts employed, and the intricacies of both the training and evaluation processes for our implementation.

D.1 Metrics

We employ the `pycocoeval` package from the `coco-caption` repository to compute CIDEr [39]. For CIDEr, we adopt the default parameters of $n = 4$ and $\sigma = 6$, as outlined in [39]. However, for Rouge-L [26], a widely utilized metric in the Natural Language domain, we utilize a more convenient package available from Hugging Face. The Rouge-L metric can be accessed through the following link: `evaluate-metric/rouge`. When configuring Rouge-L, we set the input arguments as `use_aggregator=True` and `use_stemmer=True`, following the default setup. It’s important to note that before computing the metrics, both the predicted text and the ground-truth text undergo transformation to lowercase and are stripped of punctuation.

To compute the Retrieval-based metric (R@k/N), we followed the methodology introduced in [14]. Furthermore, this metric is complemented by BerScore [46], and for score consistency, we utilize the following hash code: `roberta-large_L17_noidf_version=0.3.12(hug_trans=4.30.2)-rescaled`. This hash code specifies the BERT model version and the Hugging Face version.

D.2 Natural Language Prompting

In order to enable the Audio Description functionality within our model, we employ the same prompting methodology as developed in LLaMA Adapter [11]. As a result, the comprehensive prompt utilized for Audio Description generation is as follows: **“Below is an instruction that describes a task. Write a response that appropriately completes the request”**. Subsequently, we include the following instruction: **“Generate a caption for this video”**. The entire prompt is depicted in Figure S7.

Below is an instruction that describes a task
 ### Instruction:
 Generate caption of this video.
 ### Response:

Figure S7: **Prompt for Audio Description Generation** The caption provided outlines the prompt utilized to activate the functionality of Audio Description generation employing the LLaMA model.

D.3 Dataset Split

As MADv2 lacks a validation set, we curated a subset of 1010 moments from two movies, 3034_IDES_OF_MARCH and 3074_THE_ROOMMATE from the Unnamed version for our ablation studies and model selection. All models and experiments were assessed under consistent parameters to ensure fair comparisons. However, Table 1 in the main paper was generated using the entire dataset in the named version to maintain parity with other baselines.

D.4 Training Protocol

The training procedure for our Audio Description Generation model strictly followed the prescribed protocol outlined in [11]. Initially, a preliminary training phase was conducted, with a sole focus on aligning the audiovisual features. This crucial step ensured the synchronization and coherence between the audio and visual elements of the input data. Subsequently, the model derived from this phase was utilized to resume training, with a specific emphasis on training the bias and gate layers as proposed in [11] for LLaMA [37] 7B architecture, in conjunction with the audiovisual encoder. In the following training phase, we did back-propagation the specified layers mentioned above. This was aimed at improving the model’s performance in generating Audio Descriptions.

The entire training process spanned over 20 epochs, during which the best model in our validation subset was selected. This process involved the meticulous selection of hyperparameters, including a learning rate of $1e - 4$, a weight decay of 0.05, and a batch size of 256. The AdamW optimizer was employed to effectively optimize the model parameters. During the alignment process, we train the audiovisual and adapter layers for 2 epochs while keeping the remainder frozen to facilitate smoother convergence and alignment of the audiovisual features. It is noteworthy that throughout the entire training regimen, the LLaMA model remained frozen, thereby preserving its integrity and preventing inadvertent alterations to its pre-trained parameters.

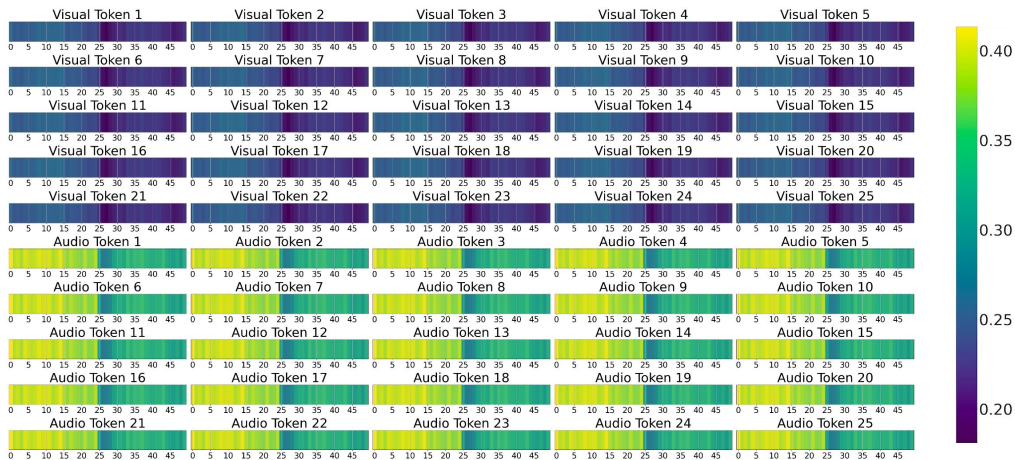


Figure S8: **Analysis of LAM Failure Example in Audio Description Generation.** This plot shows the learnable mask (LAM’s output) from the example in Figure 3, with the visual features remaining the same but the audio tokens corresponding to the last 25 samples from the movie’s credits that only include soundtrack. While the visual part assigns low values appropriately, the audio part fails to choose appropriate values, assigning mid-range values from the distribution. Note that video tokens are represented on the x-axis from 0 to 24, while audio tokens range from 25 to 50 on the same axis.

E Qualitative Analysis

Figure S8 illustrates a failure case of our Learnable Attention Mask (LAM) method. In this example, we use the same visual information as Figure 3 of the main paper, but the audio samples correspond to 25 tokens from the credits section, containing only *soundtrack music*. Although LAM successfully assigns minimal values to the visual tokens, indicating its ability to recognize the lack of relevance between the video and audio tokens, it fails to handle the audio tokens appropriately. Instead of assigning values close to zero for the audio tokens, which would be the desired behavior, LAM assigns intermediate values from the distribution, suggesting a misinterpretation of the audio information's significance.